

**ES2007-36154**

## **SOLAR DISH FIELD SYSTEM MODEL FOR SPACING OPTIMIZATION**

**John Igo**  
**Charles E. Andraka**  
Sandia National Laboratories  
Albuquerque, NM, 87185-1127, USA

### **ABSTRACT**

Dish Stirling power generation systems have been identified by DOE, Sandia National Laboratories, and Stirling Energy Systems (SES) as having the capability of delivering utility-scale renewable energy to the nation's electrical grid. SES has proposed large plants, 20,000 units or more (0.5 GW rated power) in one place, in order to rapidly ramp up production automation. With the large capital investment needed in such a plant it becomes critical to optimize the system at the field level, as well as at the individual unit level.

In this new software model, we provide a tool that predicts the annual and monthly energy performance of a field of dishes, in particular taking into account the impact of dish-to-dish shading on the energy and revenue streams. The Excel-based model goes beyond prior models in that it incorporates the true dish shape (flexible to accommodate many dish designs), multiple-row shading, and a revenue stream model that incorporates time-of-day and time-of-year pricing. This last feature is critical to understanding key shading tradeoffs on a financial basis. The model uses TMY or 15-minute meteorological data for the selected location. It can incorporate local ground slope across the plant, as well as stagger between the rows of dish systems. It also incorporates field-edge effects, which can be significant on smaller plants. It also incorporates factors for measured degraded performance due to shading.

This tool provides one aspect of the decision process for fielding many systems, and must be combined with land costs, copper layout and costs, and O&M predictions (driving distance issues) in order to optimize the loss of power due to shading against the added expense of a larger spatial array.

Considering only the energy and revenue stream, the model indicates that a rectangular, unstaggered field layout maximizes field performance. We also found that recognizing and accounting for true performance degradation due to shading significantly impacts plant production, compared with prior modeling attempts.

### **INTRODUCTION**

Stirling Energy Systems, with support from DOE and Sandia National Laboratories, is planning to commercialize dish-Stirling technology at a utility scale. They have signed power purchase agreements with two major utilities for installations up to 900MW (36,000 units) in one place [1]. In prior efforts by other companies, the

deployment model was remote off-grid or end-of-line support, with very small fields of dishes or single dishes. In these cases, the "system" was defined as a stand-alone dish-engine combination. However, with the SES mode of deployment, we need to expand the definition of "system" to include the entire field, taking into account the interactions between systems within the field.

One of the key interactions within the field-wide system is shading. This can have a tremendous impact on the energy (or revenue) production of the plant. On a small plant, shading can be eliminated by placing the dishes on a north-south line with sufficient spacing to avoid noon shading in December. However, this approach is impractical in a large plant. Therefore, recognizing that shading will be present in the morning, evening, and possibly at noon, we must have systems-level tools for making optimization decisions.

In prior work, Osborn [2] modeled shade interactions between round dishes in a small field, and created some optimized layout plans for these fields based on energy production. Several limitations will be addressed in the current work. First, the dish shape is important for detailed studies. Second, Osborn only considered a rectangular layout, and we want to see the effects of staggering the rows. Staggering rows has potential benefits from a system maintenance and access point of view, so it is desired to determine the impact or benefit of staggering on production and revenue. Figure 1 demonstrates the various stagger approaches explored. Third, the revenue is not uniform with power produced, so we want to optimize revenue rather than energy produced. Fourth, Osborn assumes that the dish would continue to produce power proportional to the illuminated area of the dish. Real data indicates that the output is reduced more rapidly than the illuminated area, and that the system cannot operate at all once a certain level of shading is attained. Less important issues that can be incorporated include ground slope, multiple-row shading and edge effects, and super-linear degradation of system performance with shading.

The shading analysis is only one part of a systems-level optimization. One must consider the cost impacts of increased spacing compared to the revenue increases. These costs may include, but are not limited to, factors such as electrical lines (wire cost, wire diameter, trenching and conduit, layout, etc.), land costs, maintenance drive times, wind impacts, etc. This model does not incorporate these cost features, but a full systems evaluation must take these into account.

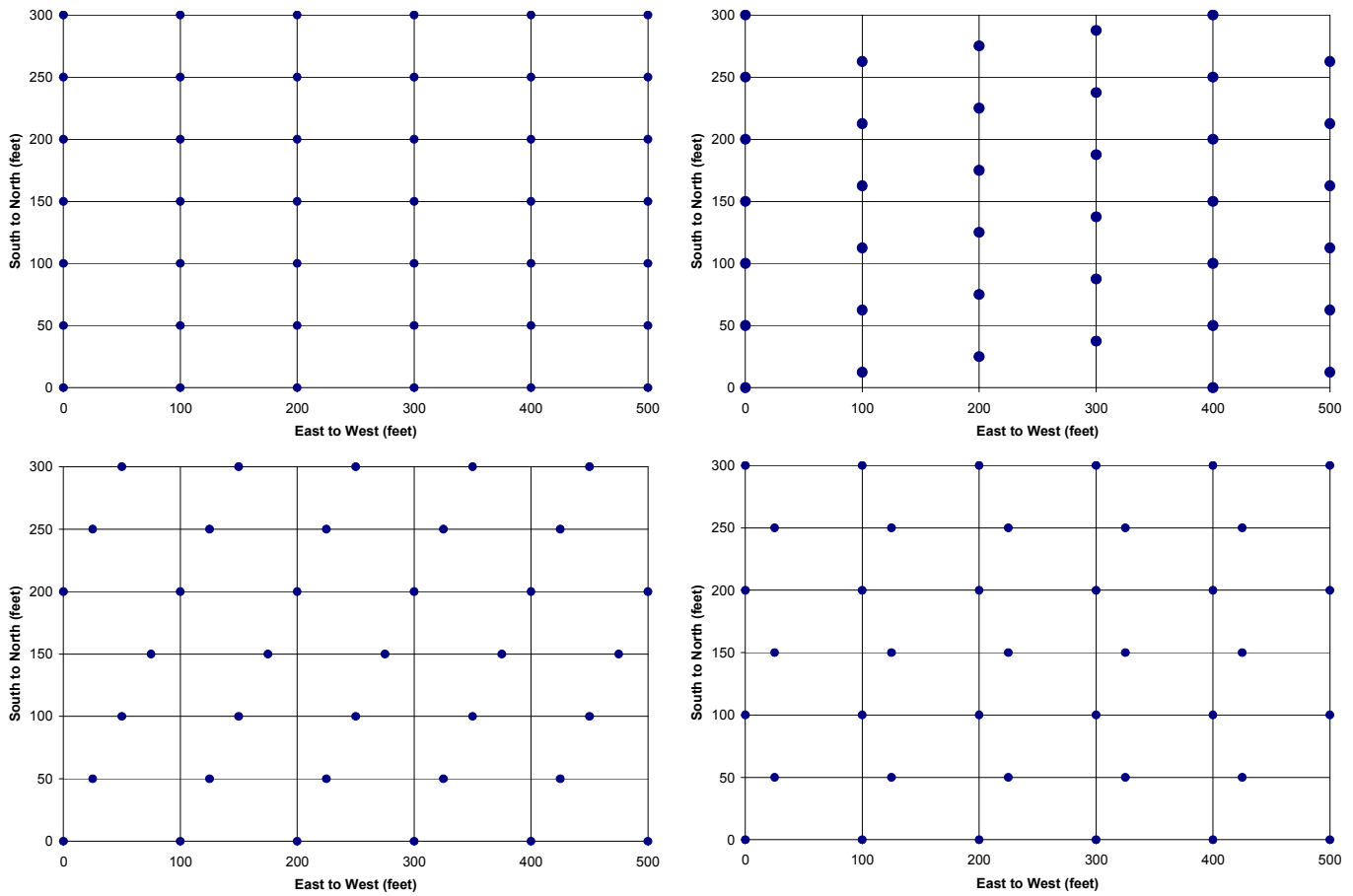


Figure 1. Stagger approaches explored in the model: a) Rectangular layout, b) North-South stagger (25% shown), c) East-West stagger (25% shown), d) East-West Herringbone Stagger (25% shown).

## MODEL APPROACH

The model was built in Excel Visual Basic for Applications (VBA), in order to provide portability to industry partners. While not the simplest development platform, anyone with Excel will be able to run and/or modify the code to suit their purposes.

The model begins with a simple linear model of Dish Stirling performance, as suggested by Stine [3], with correction for ambient temperature. While Stine corrected for cooling water temperature, existing meteorological data is based on ambient temperatures, and this is a more “systems level” approach. The model predicts system performance (net output power) vs. insolation input to the system. The simplistic model requires an input of the full rated power at 1000W/m<sup>2</sup> and the insolation level at which the system reaches 0 power (typically around 300W/m<sup>2</sup>). These two points are joined with a straight line, forming the basis for the model. This line is then adjusted in slope based on the inverse of the ambient temperature, scaled from the nominal (usually 20°C) rated condition (eq.1). Figure 2 shows this model compared to real data from the SES dish system on a clear day. Our experience has been that the output of the Stirling dish systems is accurately modeled with this temperature-corrected linear relationship. We do not account for transient effects, as the thermal and mechanical inertia of these systems is very small.

$$P = (I - I_{\min}) \cdot \frac{P_{1000}}{(1000 - I_{\min})} \cdot \frac{T_{\text{nom}}}{T_{\text{amb}}} \quad (1)$$

Where:

P=Net power produced (kW)

I=Direct Normal Insolation (W/m<sup>2</sup>)

$I_{\min}$ =Minimum insolation to operate

$P_{1000}$ =Power output at 1000W/m<sup>2</sup> (kW)

$T_{\text{nom}}$ =Nominal rated ambient temperature (K)

$T_{\text{amb}}$ =Ambient temperature (K)

We then use available meteorological data to integrate this model over a typical year for the location proposed. The most readily

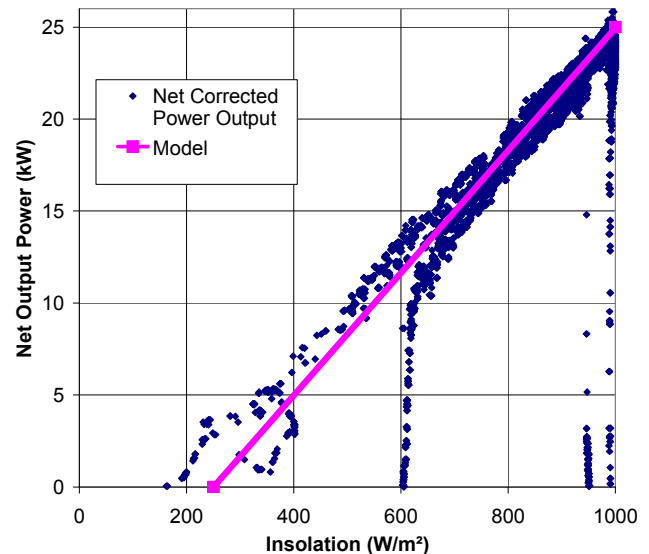


Figure 2. Linear model compared to real data for a dish-engine system.

available data is the NREL TMY2 data [4] (Typical Meteorological Year), which is a dataset of 1-hour data for a typical year. We also had 15-minute data available for the Barstow, CA location from the Solar 1 Power Tower project. While this data has a finer temporal resolution, it is only data from one actual year (1977), and has not been massaged to make it “typical.” The model reads the insolation, temperature, and wind speed each hour, calculates the energy output, and integrates this over the entire year. The wind speed is used as a “go/no-go” switch, as the dishes will stow in high winds. This approach provides the energy production for a single dish unit over the entire year.

The energy calculation can also be multiplied by a table of revenue values for the time-of-day and time-of-year value of the energy produced. It is typical in a large plant that the utility will provide greater revenue, often over a factor of 3 in the summer afternoons, as compared to the rest of the year. This is a published multiplier rate, and can dramatically impact the cost/benefit optimization. The revenue multiplier may be less than 1 at other times (Winter, nights) to balance the summer rates. Our model has a table with 24 hour rows and 12 month columns. Finer granularity could be incorporated, including the effects of weekends and holidays. However, the benefit would be limited by other uncertainties in the model, such as the TMY2 data. The model runs presented use an arbitrary but realistic rate multiplier table to demonstrate the impact.

This simple model is then modified for shading, average cleanliness, shading degradation, and other factors. The shading is based on a “typical” dish in the center of the field, and will factor in blockage for multiple interfering dishes as needed to accurately predict the shade. In addition, the model accounts for “edge effects”, with a user-settable number of edge-of-field dish rows that are treated differently. This is a small effect on a large field, but can be significant on a field of only a few MW.

The Excel spreadsheets that contain the output datasets are then used to plot the information, including monthly and annual energy and revenue, shading reduction of energy and revenue, and other insights. In addition, we built the model to accept “loop” parameters for any given input. This can be used, for example, on dish spacing, to vary the parameter over a range and then plot the impact on energy or revenue. This provides a simple mechanism to make a large number of runs to explore optimization.

## SHADING MODEL DETAILS

The shading impact is implemented by reducing the energy input (insolation) by the fraction of the dish that is shaded, effectively shifting the performance curve downward. The shading degradation factor allows us to further reduce the performance of the system, beyond the proportional reduction through shading. This is necessary because in a multi-cylinder engine, the shading typically impacts only one or two cylinders, and thus the engine runs in an unbalanced condition. Experimental data indicates the shading has a greater-than-proportional effect. The degradation factor also further shifts the performance curve (equation 2). When a specified maximum percentage of shading is reached, the dish output is set to zero, as the imbalance in cylinder power exceeds the capabilities of the engine controls and the system is taken offline. Figure 3 shows the impact of shading on the performance curves.

$$I_{\text{mod}} = I \cdot C \cdot (1 - s \cdot d) \quad (2)$$

Where:

$I_{\text{mod}}$  = Modified Direct Normal Insolation (W/m<sup>2</sup>)

$I$  = Direct Normal Insolation (W/m<sup>2</sup>)

$C$  = Cleanliness Factor (fraction, 1=fully clean)

$s$  = Shading (fraction, 0=no shade, 1=full shade)

$d$  = Shading Degradation Factor (1.6 = 60% degradation)

Note:  $s \cdot d$  must be less than 1, otherwise set  $I_{\text{mod}}=0$ .

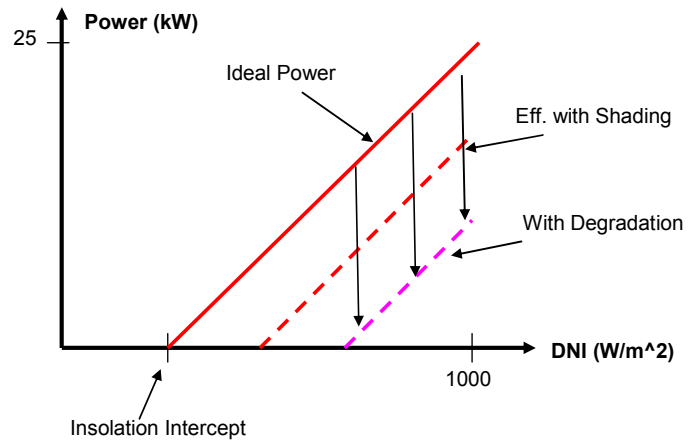


**Figure 3. Impact of shading and shading degradation factor on the system performance curve.**

Based on the sun elevation, we determine the “circle of influence”, or the number of rows and columns of dishes that can have an impact on the representative interior dish. We build a “mini field” containing this number of rows and columns, and place the representative dish in the corner of the field opposite the sun position. This mini field may include only one dish if there is no influence of shading, and may include several rows and columns of dishes if the sun is low in the sky. Then the line of sight of the dish to the sun is calculated, and only those dishes in the line of sight are considered for shading. We assume that all dishes are operational and on sun, and we do not account for fixed shading objects. Figure 4 shows a field layout with stagger, and the dishes that fall in the line-of-sight of the representative dish.

Each dish is then divided into vertical strips, or “chunks.” On the representative dish, these are called “primary chunks”, and on all of the potential shading dishes these are “secondary chunks.” The vertical strips allow us to model a variety of dishes with Cartesian layouts. A circular dish could be represented with a larger number of vertical strips, or the model revised to allow curved edges. Figure 5 shows the chunks on the participating dishes, and shows the shading chunks for a given primary chunk.

The corners of the secondary chunks are projected onto the primary chunk, resulting in possibly several overlapping shadows. Once all shadows are determined on a primary chunk, they are sequenced by the height of the top edge of the shadow, highest first (Fig. 6a). The shadows are then trimmed to the size side-to-side of the primary chunk (Fig. 6b). Starting from the highest shadow, all shorter shadows are truncated side-to-side to the sides of the taller shadow

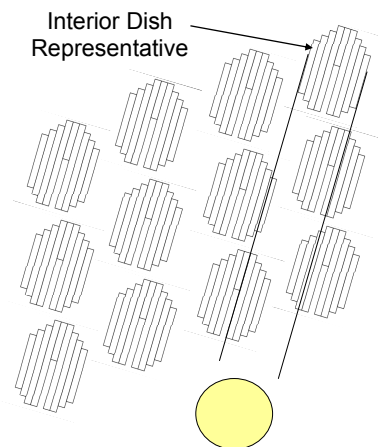


**Figure 4. Field layout with stagger, showing dishes within the “circle of influence” and line-of-sight.**

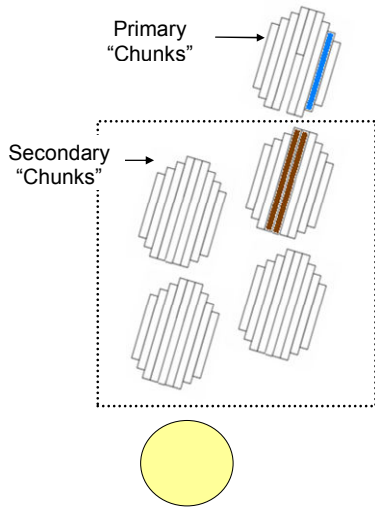


**Figure 5. Primary chunks shown on primary dish, with participating secondary chunks highlighted on the secondary dishes.**

(Fig. 6c). This process is repeated for all shadows (Fig. 6d). This results in a single-layered shadow on the primary chunk. This process is repeated for each primary chunk. Finally, the total area of shadow is added up on the dish, and compared to the total area of the dish.

The shadowing changes far more rapidly than the meteorological data available. Therefore, the sun position is incrementally determined between the meteorological data points using NREL's SOLPOS routine [5]. At each of these sub-increments of time, the power of the dish is calculated. The incremental power is then integrated over the meteorological timestep. If no shading is detected in a timestep, then the power is calculated once for the whole timestep. The shading degradation factor is applied to the shaded area, further reducing power. If the shading, before degradation, exceeds the maximum shading allowed (input parameter), the output power is set to zero.

Depending how many perimeter rows (edge effects) are specified, the calculations are re-run for the special cases on the edges exposed to the sun direction. For example, before noon in the winter, the East

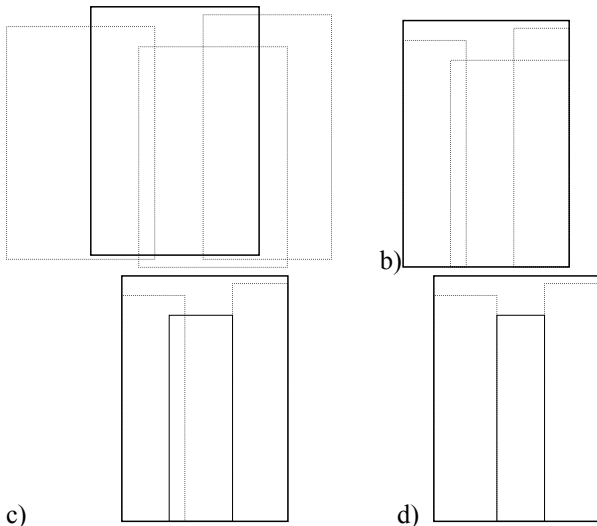


**Figure 6. Progression of overlapping shade layout. a) All overlapping shade is sequenced from tallest to shortest, b) all shade is cropped to primary chunk width, c) shorter shade is cropped side-to-side by tallest shade, and d) Each taller shade crops any shorter shade, resulting in final one-layer shade profile.**

and South edges of the field are considered as special cases. The number of rows to be considered as special can be specified. More rows will result in finer detail, but at the expense of more computation.

At each increment of time, the value of the energy is determined from the lookup table and multiplied by the energy generated.

The program can also account for a field-wide slope of the terrain, but not local changes in slope. This may enhance or decrease shading.

## RESULTS

In order to verify the shading model, the shadow pattern on one dish was carefully measured at several instances near the winter solstice. This was then qualitatively compared to the graphic output provided by the model. The results indicated the model accurately predicts the shape of the shadow on neighboring dishes. Figure 7 shows one such comparison. A number of these comparisons give us a high degree of confidence that the shading model is working correctly.

We looked at existing operational data on several clear days in the winter. First, we found the controller typically declared a fault based on the cylinder power imbalance when the shading reached 10.5%. At this point, if only one cylinder's portion of the reflected light at the receiver is blocked, over 40% of that cylinder's power is missing, causing a strong imbalance in the engine temperatures. Second, we compared the data from a shaded dish to an unshaded dish on a clear day (Fig. 8) and determined that for these systems a shading degradation factor of 1.6 (60% additional power lost) matched the data. The raw efficiency is calculated based on the dish area, the Direct Normal Insolation, and the power output. Then the shade percentage, calculated with the subject model, is used to modify the efficiency by decreasing the dish area by the percentage of shading. The plot of this shade-modified efficiency still shows a decrease in performance due to the shading, when compared to an unshaded dish that has nearly flat efficiency throughout the middle of the day. Finally, the shade enhancement factor was included, increasing the effective amount of shade in the efficiency calculation. This factor was varied until the mid-day modified efficiency was relatively flat (visual observation).

For this paper, we modeled a representative field of 20,000 dish systems in Barstow, CA, using the 15-minute 1977 meteorological data from the Solar One Central Receiver Project [6,7] project. The dishes were laid out in a grid 160 dishes wide (East to West) and 125 dishes high (North to South). We did not degrade dish performance for cleanliness. We assumed full rated net power (25kW) at 1000 W/m<sup>2</sup> insolation, and zero rated net power at 250 W/m<sup>2</sup>, at 20°C nominal ambient temperature. The stow wind speed was set to 30 MPH. We nominally assume the spacing to be that of the Model Power Plant in Albuquerque [8], or 52 feet North to South and 104 feet East to West, and then varied from this condition for our optimizations.

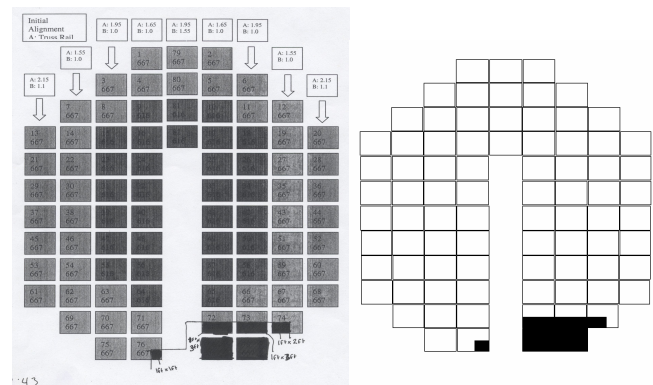


**Figure 7. Shade prediction compared to measured field data. Many such comparisons were performed to validate the model.**

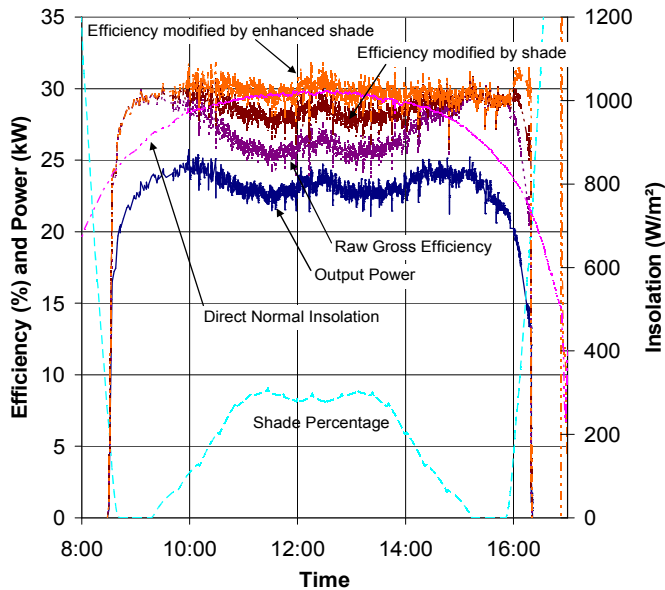


**Figure 8. The Gross Efficiency Raw uses the entire area of the dish. The insolation used in the efficiency calculation was then modified by the shade percentage, and then the shade degradation factor was varied until the efficiency curve was nearly flat through the mid day period, simulating observations on an unshaded dish (south row) on the same day. The resulting shade degradation factor was 1.6.**

We used a simple model of the revenue stream, with \$0.10/kW-hr at most times. During summer months (June, July, and August) we arbitrarily increased the value to \$0.30/kW-hr from noon to 7pm. During the winter months of December, January, and February we reduced the value to \$0.06/kW-hr. These values were selected to visually differentiate the difference between revenue and energy in these models. However, actual negotiated contracts with utilities will be different, and will affect the revenue-optimized results. The actual negotiated values are often not publicly known.

Based on these assumptions, the field produced 1072 GW-hr for the year, and the revenue produced was \$138M. This can be compared to the production possible with an unshaded system (impossible at these scales) of 1156 GW-hr and \$146M, or a loss of 7.3% of the energy and 5.5% of the revenue due to the shading. If we modify the model to ignore shading degradation, and allow operation to continue proportional to shading up to 100% shading, simulating the Osborn model, the production is 1111 GW-hr and \$142M. Therefore, we can see the impact of the recorded effects of dish shading over the Osborn model amount to an additional loss of 3.5% of energy and 2.8% of revenue. Figure 9 shows the shading at the Winter Solstice on the typical dish. Shading is clearly seen in the morning and evening, as well as mid-day shading from the close North-South dish spacing employed at the Model Power Plant.

We then put this model to work on the primary task that inspired this development, staggering the field layout. The proposed changes to the layout would possibly reduce mid-day winter shading and improve service access. When a south dish is serviced in the north, face-down position (a safe position to avoid concentrated light on the grass), truck access is difficult without also removing the next northward dish from service.

Figure 10 and Fig. 11 indicate that there is a reduction of energy production (and revenue) when the field is staggered. This is because as the sun travels to either side of due south, it is lower in the sky, and more shading occurs rather than less. These calculations were performed with the dishes spaced 52 feet north to south and 104 feet

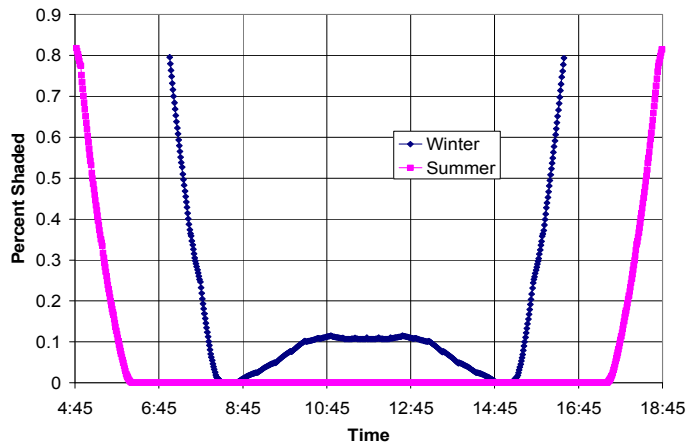


**Figure 9. Dish shading on the Winter and Summer Solstices, showing shading from neighboring dishes East and West (morning and evening) and North to South (mid day Winter).**

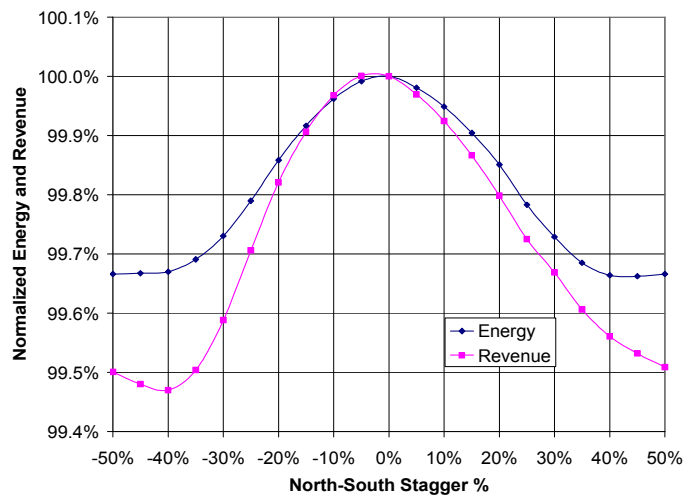


**Figure 10. Effect on Energy and Revenue while varying north to south stagger. The energy and revenue are normalized to the values generated without any stagger.**

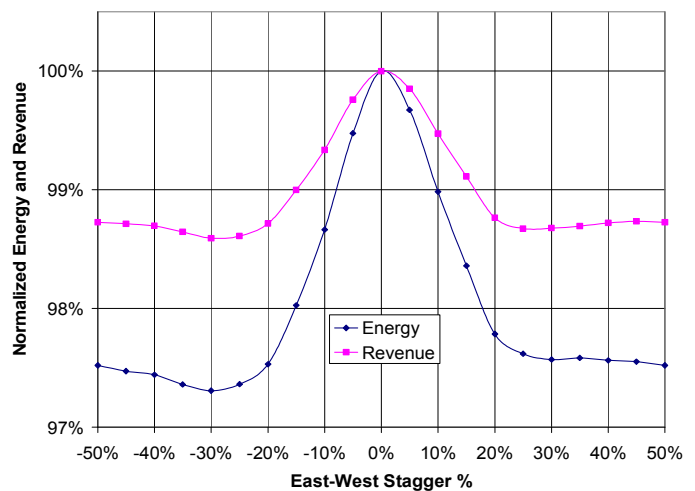


**Figure 11. Effect of varying east to west stagger on revenue and energy production. Again, the values are normalized to the energy and revenue generated without stagger. A larger effect is noted here for E-W stagger than for N-S stagger.**

east to west, the layout of the Model Power Plant. While the degradation may appear small, the 1.4% revenue loss in the East-West stagger case amounts to nearly \$2M annual loss. From this work, we have determined that it is best to lay the field out in a rectangular, unstaggered grid. The model was run with 20,000 dish systems, so edge effects are minimal. The energy produced at the unstaggered condition is about 1073GW-hr, or revenue about \$138M/year. Notice that the north-south stagger has a smaller overall effect, and that the impact is greater on revenue than energy. This is because the increased losses occur in the morning and evening, and there is a substantial financial benefit in the summer evenings. The east-west stagger has a greater overall impact. However, the impact on revenue is far less than that on energy production, because the impact is primarily during the winter when the value of electricity is lower.

We then varied the n-s and e-w dish spacing. Figure 12 shows the effect of north to south spacing while the east to west spacing is held at 104 feet without stagger. The sharp inflection in the curve is when the mid-day winter shading ceases to cause the system to go offline at mid day in the winter. The impact on revenue is not as great, as the revenue model used gives a strong benefit (3x) to the afternoon summer hours. We determined initially that the spacing should be increased to the point just beyond the inflection, or increased from 52 feet to at least 54 feet. Further increases have a smaller payoff, but may still be cost effective, depending on the value of land, wiring, and maintenance.

With this new spacing (55 feet, no stagger was selected), we varied the east-west spacing. The impact is less dramatic, as seen in Fig. 13. Prior work reported by Osborn suggests a 2:1 ratio between E-W and N-S spacing, which would put the modified spacing at 110 feet E-W.

## CONCLUSIONS

We developed an energy and revenue stream model of a large field of dish Stirling systems, part of a suite of tools to optimize the cost/benefit ratio of such a system. This model extends past work by including the real dish shape, the revenue model, row stagger, multiple rows of shading providers, and general terrain slope. The energy model is based on the recognized Stine model, with modifications to the shading based on real data. A primary motivation of this model was to evaluate the impact on shaded performance of staggering the field layout for maintenance reasons.

We found that the optimum layout of a dish field, considering only the revenue and energy streams, is a rectangular grid without stagger. We also found that a slight increase in field spacing can develop considerably more revenue by avoiding trip-outs mid-day in the winter months.

This model is only a part of the equation for field optimization. Additional factors include land cost, wiring costs, and O&M travel time. However, this tool is flexible and can be used as part of the decision process in developing field layout.

## ACKNOWLEDGMENTS

Sandia is a multiprogram laboratory operated by Sandia Corporation, a Lockheed Martin Company, for the United States Department of Energy's National Nuclear Security Administration under contract DE-AC04-94AL85000. Stirling Energy Systems provided access to data and system operation of their 6-dish Model Power Plant at Sandia National Laboratories in Albuquerque NM.

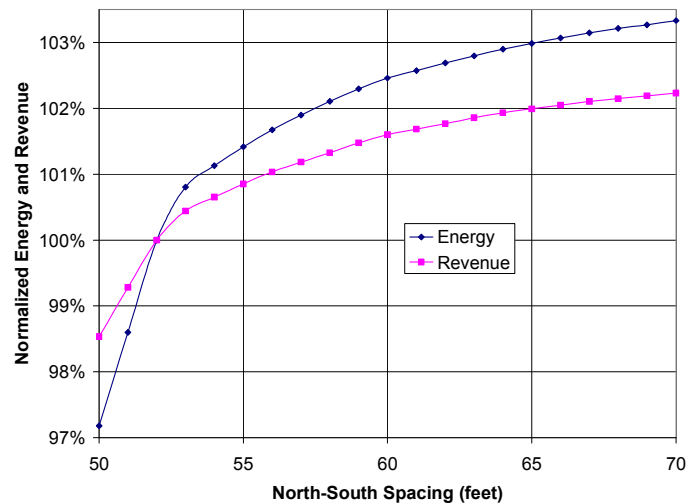


**Figure 12. Effect on revenue and energy production of variations in north to south dish spacing. Strong inflection in the curve is when shading ceases to cause system shutdown. The results are normalized to the energy and revenue produced at 52 feet spacing, the layout of the present 6-dish development plant in Albuquerque, and the field is not staggered.**

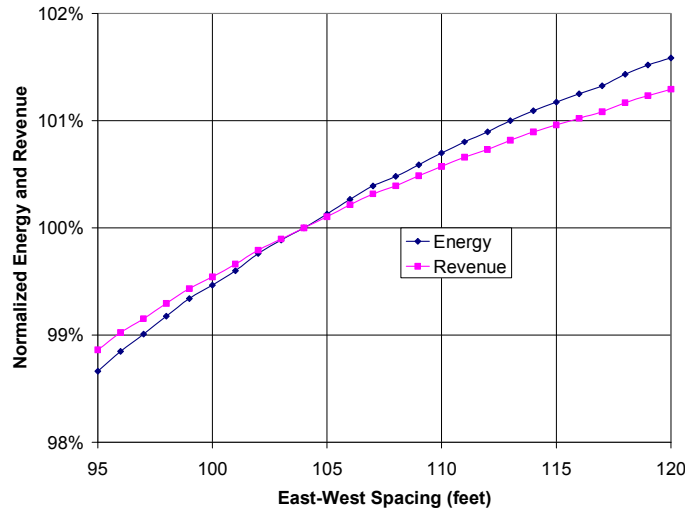


**Figure 13. Effect on revenue and energy production of variations in East to West dish spacing. The results are normalized to the energy and revenue produced at 104 feet E-W spacing, the layout of the present 6-dish demonstration plant in Albuquerque, and the field is not staggered.**

## REFERENCES

- [1] Stirling Energy Systems, 2005, [http://www.stirlingenergy.com/breaking\\_news.htm](http://www.stirlingenergy.com/breaking_news.htm), press releases announcing contracts with SDGE and SCE.
- [2] Osborn, D.B., 1980, "Generalized Shading Analysis for Paraboloidal Collector Fields", Paper Number 80-Pet-33, American Society of Mechanical Engineers, New York, NY, presented at the ASME Energy Technology Conference & Exhibition, New Orleans, LA, February 3-7, 1980.

- [3] Stine, W.B., 1995, "Experimentally Validated Long-Term Energy Production Prediction Model for Solar Dish/Stirling Electric Generating Systems", Paper Number 95-166, *Proceedings of the Intersociety Energy Conversion Engineering Conference*, D.Y. Goswami, L.D. Kannberg, T.R. Mancini, S. Somasundaram, eds., American Society of Mechanical Engineers, New York, NY, **vol. 2**, pp. 491-495.
- [4] Marion, W., K. Urban, 1995, "User's Manual for TMY2s, Typical Meteorological Years", National Renewable Energy Laboratory, Golden, CO.
- [5] 2000, "NRELS's SOLPOS 2.0: Documentation", National Renewable Energy Laboratory, Golden CO,  
<http://rredc.nrel.gov/solar/codesandalgorithms/solpos/aboutsolpos.html>.
- [6] Stoddard, M.C., Faas, S.E., Chaing, C.J., Dirks J.A., 1987, "SOLERGY – A Computer Code for Calculating the Annual Energy from Central Receiver Power Plants", SAND86-8060, Sandia National Laboratories, Albuquerque, NM.
- [7] Randall, C. M., 1978, "Barstow Insolation and Meteorological Data Base". ATR-78(7695-05)-2, The Aerospace Corporation., El Segundo, CA.
- [8] Andraka, C.E., 2005 "Performance of Six SES Dish Engine Units", *Solar Power 2005 Conference*, Solar Electric Power Association, Washington DC.